

# Unconventional phonon blockade via atom-photon-phonon interaction in hybrid optomechanical systems

Mei Wang,<sup>1,2</sup> Xin-You Lü,<sup>1,\*</sup> Adam Miranowicz,<sup>3,2</sup> Tai-Shuang Yin,<sup>1</sup> Ying Wu,<sup>1,†</sup> and Franco Nori<sup>2,4</sup>

<sup>1</sup>*School of physics, Huazhong University of Science and Technology, Wuhan 430074, China*

<sup>2</sup>*Theoretical Quantum Physics Laboratory, RIKEN Cluster for Pioneering Research, Wako-shi, Saitama 351-0198, Japan*

<sup>3</sup>*Faculty of Physics, Adam Mickiewicz University, 61-614 Poznań, Poland*

<sup>4</sup>*Department of Physics, The University of Michigan, Ann Arbor, Michigan 48109-1040, USA*

(Dated: June 12, 2018)

Phonon nonlinearities play an important role in hybrid quantum networks and on-chip quantum devices. We investigate the phonon statistics of a mechanical oscillator in hybrid systems composed of an atom and one or two standard optomechanical cavities. An efficiently enhanced atom-phonon interaction can be derived via a tripartite atom-photon-phonon interaction, where the atom-photon coupling depends on the mechanical displacement without practically changing a cavity frequency. This novel mechanism of optomechanical interactions, as predicted recently by Cotrufo *et al.* [Phys. Rev. Lett. **118**, 133603 (2017)], is fundamentally different from standard ones. In the enhanced atom-phonon coupling, the strong phonon nonlinearity at a single-excitation level is obtained in the originally weak-coupling regime, which leads to the appearance of phonon blockade. Moreover, the optimal parameter regimes are presented both for the cases of one- and two- cavities. We compared phonon-number correlation functions of different orders for mechanical steady states generated in the one-cavity hybrid system, revealing the occurrence of phonon-induced tunneling and different types of phonon blockade. Our approach offers an alternative method to generate and control a single phonon in the quantum regime, and has potential applications in single-phonon quantum technologies.

PACS numbers: 42.50.Vk, 37.10.Vz, 37.90.+j

## I. INTRODUCTION

Quantum effects in cavity optomechanical systems [1–6] and nanomechanical resonators (NAMRs) [7–10] have attracted extensive attention and progressed enormously in the past several years. Reaching the quantum limits of optomechanical systems is relevant for implementing single-photon and single-phonon devices for quantum metrology [11, 12] and quantum information processing [13–15]. To explore quantum effects of photons, many theoretical studies (for a recent review see [16]) have been focused on the nonlinear quantum regime, where a single-photon nonlinearity is comparable to a cavity decay. These studies were devoted, in particular, to conventional [17–19] and unconventional [20–23] photon blockades, which are optical analogues of Coulomb blockade.

However, observing quantum effects in NAMRs becomes more complex. The main obstacle is the thermal environment, which affects the coherence and induces dissipation of NAMR states. In general, if a NAMR is cooled to its ground state at low temperatures and the frequency of the NAMR is high enough (of several GHz), then the oscillations of the NAMR quanta can beat the thermal energy and approach the quantum limit. Even so, exploring purely quantum phenomena for phonons is still very challenging, such as the generation and detection

of phonon blockade [24–30], the generation of nonclassical states of phonons [31, 32], including squeezed phonon states [33–36] and Schrödinger-cat states [37]. Strong phonon nonlinearities become necessary in order to explore the quantum behavior of NAMRs. To satisfy this condition, NAMRs are often coupled to an artificial atom (or a qubit) to form a hybrid system [16, 38–48]. Such hybrid systems, with atom-phonon-interactions, have obvious advantages for inducing strong phonon nonlinearities compared to standard systems with phonon-phonon interactions [49, 50] and photon-phonon interactions [51–53].

To realize such atom-phonon interactions [54], different theories and experimental methods have been presented [46, 55, 56]. Strong phonon nonlinearities can be obtained through a NAMR coupled directly to an artificial atom, but it is difficult to be engineered and dynamically controlled [57, 58]. Recently, Cotrufo *et al.* [59] predicted a novel mechanism of optomechanical interactions, which enables the indirect enhancement of the phonon nonlinearity via an atom-photon-phonon (tripartite) interaction. This effect, which is referred to as *mode field coupling*, corresponds to “a fundamentally different situation in which the mechanical displacement induces a variation of the spatial distribution of the cavity field, while cavity frequency is negligibly affected” [59]. In other words, this mechanical displacement modifies the cavity-field distribution which, in turn, modulates the atom-phonon interaction. With this strong controllable nonlinear interaction, many phenomena can be explored, including phonon blockade and phonon-induced tunnel-

\* xinyoulu@hust.edu.cn

† yingwu2@126.com

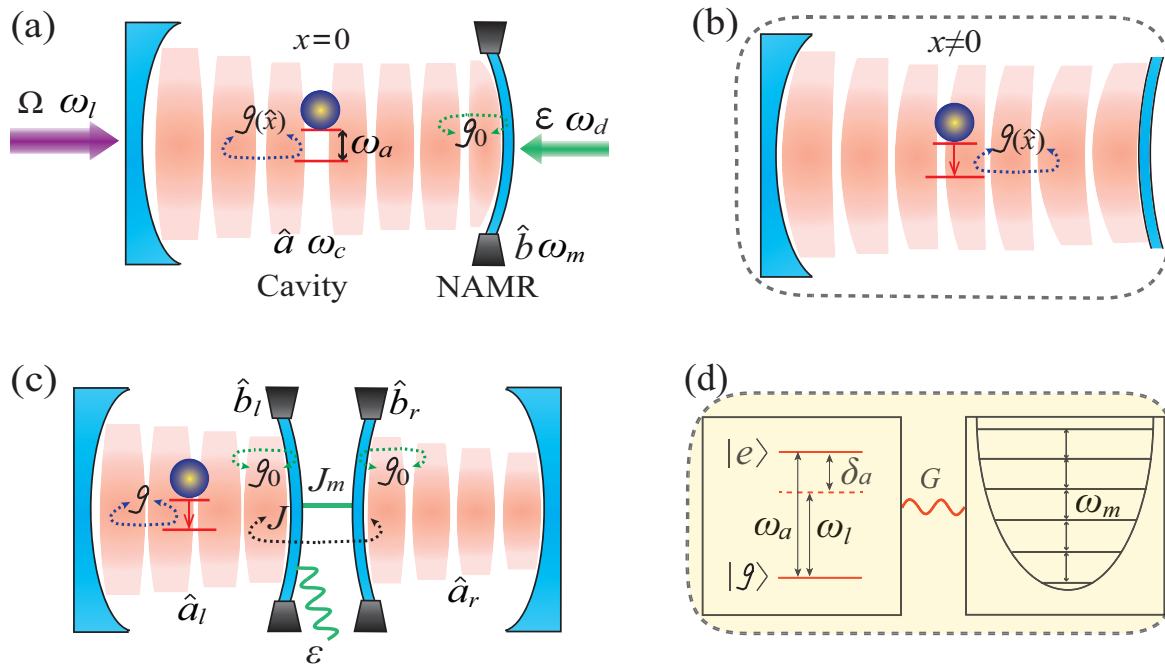


FIG. 1. (Color online) (a) Schematic illustration of a single-cavity hybrid optomechanical system, in which a two-level atom is coupled to the cavity mode  $\hat{a}$  of an optomechanical system. The photon distribution in the cavity defines an electric field, which is zero at the position of the atom when the displacement  $x = 0$ . To demonstrate quantum effects of the hybrid optomechanical system, a strong driving field  $\Omega$  with frequency  $\omega_l$  and a weak pumping field  $\epsilon$  with frequency  $\omega_d$  act on the cavity mode (field  $\hat{a}$  and frequency  $\omega_c$ ) and the NAMR (with field  $\hat{b}$  and frequency  $\omega_m$ ), respectively. (b) Due to the displacement of the NAMR at the cavity boundary, the electric-field distribution at the atomic position becomes dense and induces an atomic radiative transition. (c) A two-cavity hybrid optomechanical system, where two standard optomechanical cavities are coupled together, while a two-level atom is directly coupled to the left cavity only. The two partially-transparent movable mirrors (NAMRs) are in the middle, coupled to each other with coupling rate  $J_m$ . The left NAMR is driven by a driving field  $\epsilon$  with a resonant frequency  $\omega_m$ . (d) The energy-level diagram of the reduced model for the hybrid optomechanical systems in panels (a) and (c). In a rotating frame, the atom couples to the NAMR with strength  $G$ , which is controllable and plays a central role in these hybrid optomechanical systems.

ing in relation to their photonic analogues along the lines of, e.g., Refs. [60–62].

Phonon blockade (PB) [38] refers to a quantum nonlinear process, in which a single phonon of a nonlinear mechanical resonator blockades the excitation of another phonon. This is a close analogue of photon blockade [17–19], which refers to a process when a single photon in a nonlinear cavity blockades the entry of another photon. Note that a Kerr-type mechanical nonlinearity can simply be realized with a linear NAMR coupled to a qubit in a Jaynes-Cummings-type model far-off resonance (i.e., in its dispersive limit) [38].

In systems which are more complicated than the above-mentioned one, PB can occur as a result of multipath interference. This effect is referred to as unconventional PB (UPB), to emphasize this new mechanism of its generation. UPB was predicted for, e.g., two coupled NAMRs with two qubits [24] and a coupled qubit-NAMR-cavity system [30]. This UPB is a direct analogue of unconventional (or anomalous) photon blockade, which was first predicted in Refs. [20–22] and then explained in

terms of multipath interference in Ref. [23] (for recent reviews see Refs. [16, 63]). Unconventional photon blockade can occur for surprisingly *weak* nonlinearities (even in the *weak*-coupling light-matter regime) and still enables very *strong* photon antibunching, as described by the second-order correlation function  $g^{(2)}(0) \approx 0$  [22]. Analogously, very strong *phonon* antibunching can be predicted for UPB, as studied, in particular, here. We note that the terms of unconventional photon and phonon blockades are *not* only used to refer to blockade in the weak-coupling regime (and, thus, for weak nonlinearities). Indeed, these are also used for the strong-coupling regime [23].

The term UPB has also another meaning [64], which refers to unconventional properties of the generated field via PB (as explained in Sec. V), rather than to an unconventional mechanism for creating PB or improving its quality.

Here we investigate UPB [24] in a hybrid optomechanical system featuring a controllable atom-phonon interaction obtained from atom-photon-phonon interac-

tions [59]. Physically, this interaction results from a mechanically-induced modification of the optical field distribution, which directly determines the electric-field distribution around the atom. This leads to an atom-photon displacement-dependent interaction generating an atom-phonon interaction with an effective coupling rate  $G$  ( $G'$ ). By applying a *strong* external driving field to the cavity and a *weak* driving field to the NAMR, one can effectively control the interaction between the atom and the NAMR. Thus, it is possible to explore *single-phonon* phenomena by utilizing such atomic nonlinearity. With realistic parameters, we find analytically and numerically an optimal regime for phonon blockade.

Moreover, we also study atom-photon-phonon interaction resulting from the optomechanical interaction in a two-cavity case. This tripartite interaction and atom-phonon interaction are effectively enhanced in the two-cavity case in comparison to the single-cavity case. We also calculate the steady-state and time-variable phonon statistics. UPB is demonstrated with both original and effective Hamiltonians leading to, effectively, the same predictions. Thus, this paper offers an alternative method to generate *nonclassical phonon states through modulated atom-phonon interactions*, and can have potential applications in quantum technologies and quantum information science.

This paper is organized as follows: In Sec. II, we introduce a one-cavity hybrid optomechanical system, in which an atom couples to an optomechanical cavity mode. From the atom-photon-phonon interaction in this system, we derive the atom-phonon interaction, which is modulated by the average photon number in the cavity. This illustrates that this atom-phonon interaction is controlled by an external driving field. In Sec. III, we discuss phonon antibunching at low temperatures and give the corresponding optimal conditions for observing phonon blockade in the one-cavity system. In Sec. IV, we implement the atom-photon-phonon interaction from the optomechanical coupling in the system consisting of two coupled standard optomechanical systems. In this two-cavity system, the atom-phonon interaction is simultaneously controlled by intra-cavity photon numbers and an atom-photon-phonon interaction rate. Here we show the modulation of the atom-photon-phonon interaction rate as a function of the optomechanical coupling rate and the coupling rate of the two cavities. We also demonstrate phonon blockade in this two-cavity system. Section V presents our analysis of higher-order phonon-number correlations to reveal various types of phonon blockade and phonon-induced tunneling in the single-cavity system. Our conclusions are given in Sec. VI.

## II. ONE-CAVITY SYSTEM

We now consider a hybrid optomechanical system, which is schematically shown in Fig. 1(a). In this system, a two-level atom is coupled to an optomechanical

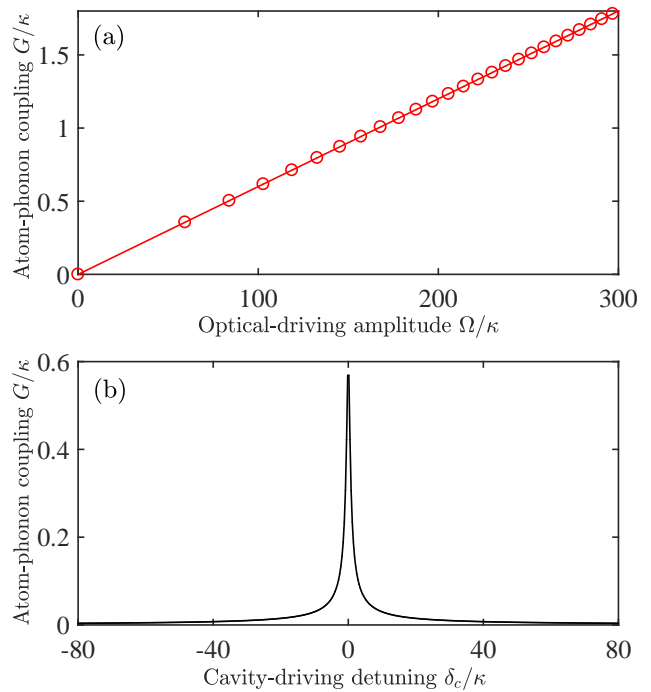


FIG. 2. (Color online) The atom-phonon coupling strength  $G = \gamma\sqrt{n_{\text{cav}}}$  versus: (a) the driving amplitude  $\Omega$  of the cavity mode with  $\delta_c = 0$  and (b) the detuning  $\delta_c$  between the cavity mode and the driving field with  $\Omega = 100\kappa$  for the one-cavity hybrid system. The parameters used here are  $\omega_c/2\pi = 470$  THz,  $\kappa/2\pi = 5$  MHz,  $\omega_m = 280\kappa$ ,  $\Gamma_c = \kappa$ ,  $\Gamma_m = 0.01\kappa$ , and  $\gamma = 0.003\kappa$ , all given in units of the atom-damping rate  $\kappa$ .

cavity, which, in turn, interacts with a NAMR with coupling rate  $g_0$ . The atom-photon coupling strength  $g(\hat{x})$  is displacement-dependent, which induces a variation of the spatial distribution of the cavity field. Simultaneously, the photon distribution around the atom determines the electric-field intensity, which induces the radiative transition of the atom. As shown in Fig. 1(b), when the mechanical displacement is  $x \neq 0$ , then  $g(\hat{x}) \neq 0$  and the atom begins the quantum Rabi oscillations between its ground and excited states. Moreover, the cavity and mechanical modes are driven by a monochromatic driving with frequency  $\omega_l$  (amplitude  $\Omega$ ) and  $\omega_d$  (amplitude  $\epsilon$ ), respectively. In a rotating frame with frequency  $\omega_l$ , the system Hamiltonian under the rotating-wave approximation can be written as [59]:

$$\begin{aligned} \hat{H}_1/\hbar = & \delta_c \hat{a}^\dagger \hat{a} + \frac{\delta_a}{2} \hat{\sigma}_z + \omega_m \hat{b}^\dagger \hat{b} + g(\hat{x})(\hat{\sigma}_+ \hat{a} + \hat{\sigma}_- \hat{a}^\dagger) \\ & + \Omega(\hat{a}^\dagger + \hat{a}) + \epsilon(\hat{b}^\dagger e^{-i\omega_d} + \hat{b} e^{i\omega_d}), \end{aligned} \quad (1)$$

where  $\hat{\sigma}_+ = |e\rangle\langle g|$  ( $\hat{\sigma}_- = |g\rangle\langle e|$ ) and  $\hat{\sigma}_z = |e\rangle\langle e| - |g\rangle\langle g|$  stand for the raising (lowering) and occupation operators of the atom with Rabi frequency  $\omega_a$ , respectively. Here  $|g\rangle$  ( $|e\rangle$ ) is the ground (excited) state of the atom. Moreover,  $\hat{a}$  ( $\hat{a}^\dagger$ ) and  $\hat{b}$  ( $\hat{b}^\dagger$ ) denote the annihilation (creation) operators of the cavity mode (with frequency  $\omega_c$ ) and

the mechanical mode (with frequency  $\omega_m$ ), respectively;  $\hat{x} = \hat{b}^\dagger + \hat{b}$  is the mechanical-mode position (displacement) operator, and the detunings  $\delta_{a,c}$  are defined by

$$\delta_a = \omega_a - \omega_l, \quad \delta_c = \omega_c - \omega_l. \quad (2)$$

In the Hamiltonian (1), we have neglected the optomechanical interaction term, because the interaction rate is usually very weak. We assume that the frequencies satisfy the condition  $\omega_a = \omega_c + \omega_m$ .

To better analyze the physical mechanism described by Hamiltonian (1), we now expand the photon-atom interaction  $g(\hat{x})$  to first order in the displacement,

$$g(\hat{x}) = g(0) + \gamma\hat{x}, \quad \gamma = \frac{dg(\hat{x})}{d\hat{x}}. \quad (3)$$

We assume that the effect of the displacement to the photon distribution disappears at the point  $x = 0$ , as depicted in Fig. 1(a), leading to  $g(0) = 0$ . Thus, substituting the above expansion into Eq. (1), we obtain the following tripartite atom-photon-phonon interaction term

$$\gamma\hat{x}(\hat{\sigma}_+\hat{a} + \hat{\sigma}_-\hat{a}^\dagger), \quad (4)$$

where  $\gamma$  is an interaction rate. This interaction is different from the standard optomechanical coupling, because the mechanical displacement changes the electric-field distribution in the cavity, which induces atomic transitions without changing the cavity frequency.

Under the conditions of strong optical driving, setting  $\delta_c = 0$ , we can obtain a large steady-state average photon number  $n_{\text{cav}}$ . The operator of the cavity field can be written in the form  $\hat{a} = \sqrt{n_{\text{cav}}} + \delta\hat{a}$ . Combined with this reshaped operator and the tripartite interaction, Hamiltonian (1) can be transformed into a driven Jaynes-Cummings-type Hamiltonian:

$$\hat{H}'_1/\hbar = \frac{\Delta}{2}\hat{\sigma}_z + \Delta\hat{b}^\dagger\hat{b} + G(\hat{\sigma}_+\hat{b} + \hat{\sigma}_-\hat{b}^\dagger) + \epsilon(\hat{b}^\dagger + \hat{b}), \quad (5)$$

in the rotating frame with frequency  $\omega_d$ , where  $\Delta = \delta_a - \omega_d$  is a detuning, and  $G = \gamma\sqrt{n_{\text{cav}}}$  is an effective Jaynes-Cummings interaction strength [24, 53, 65]. Under the condition  $\gamma \ll G \ll \omega_m$ , we have neglected the fast oscillating terms with factors  $\exp(\pm 2i\omega_m t)$  in the third term. Equation (5) illustrates the physical mechanism of the atom-phonon interaction shown in Fig. 1(d). The harmonic oscillator with frequency  $\omega_m$  is coupled to the atom, which has a shifted frequency  $\delta_a$  between the excited and ground states in the rotating frame with frequency  $\omega_l$ . Here the atom-phonon interaction  $G$  is only controllable by the photon occupation number  $n_{\text{cav}}$ , because the tripartite interaction rate  $\gamma$  is a constant in the one-cavity system. This enables us to control the atom-phonon interaction by modulating the original optical-mode driving strength. As one can see in Fig. 2, the coupling strength  $G$  is proportional to the amplitude of the driving field, while the other parameters are constant.

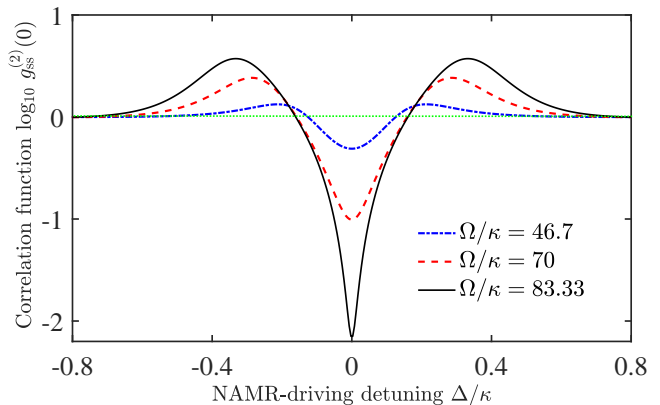


FIG. 3. (Color online) Second-order phonon-number correlation function  $g_{\text{ss}}^{(2)}(0)$  [precisely,  $\log_{10} g_{\text{ss}}^{(2)}(0)$ ] for the phonon steady states generated in the NAMR versus the detuning  $\Delta$  between the NAMR mode and the corresponding driving field with different optical driving amplitudes  $\Omega$  in the one-cavity system. Here, the thermal phonon is  $\bar{n}_{\text{bth}} = \bar{n}_{\text{ath}} = 0$  at low temperatures. The driving amplitude of the oscillator is  $\epsilon = 0.01\kappa$ , and the detuning  $\delta_c = 0$ , while all the other parameters are the same as in Fig. 2.

Furthermore, the resonant driving of the cavity can drastically strengthen the interaction strength  $G$ . These results illustrate that one can easily control and enhance the atom-phonon interaction  $G$  from the weak to strong coupling regimes and even up to the ultra-strong coupling regime. This also facilitates the system to enter the quantum regime and display quantum properties of phonons.

### III. PHONON BLOCKADE IN THE ONE-CAVITY SYSTEM

Including the dissipation caused by the system-bath coupling, the system dynamics is described by the Markovian master equation

$$\begin{aligned} \dot{\hat{\rho}} = & -i[\hat{H}'_1, \hat{\rho}] + \Gamma_m(\bar{n}_{\text{bth}} + 1)\mathcal{D}[\hat{b}]\hat{\rho} \\ & + \Gamma_m\bar{n}_{\text{bth}}\mathcal{D}[\hat{b}^\dagger]\hat{\rho} + \kappa\mathcal{D}[\hat{\sigma}_-]\hat{\rho}, \end{aligned} \quad (6)$$

where  $\mathcal{D}[\hat{o}]\hat{\rho} = \hat{o}\hat{\rho}\hat{o}^\dagger - (\hat{o}^\dagger\hat{o}\hat{\rho} + \hat{\rho}\hat{o}^\dagger\hat{o})/2$  ( $\hat{o}$  is a normal annihilation operator) is the standard Lindblad dissipative superoperator for the damping of the atom and NAMR. Here  $\kappa$  and  $\Gamma_m$  are the damping rates of the atom and the NAMR, respectively. Moreover, the thermal occupation of the atom has been ignored at very low temperatures, i.e.,  $\bar{n}_{\text{ath}} = 0$ . The thermal phonon number  $\bar{n}_{\text{bth}}$  around the NAMR follows the Bose-Einstein statistics  $\bar{n}_{\text{bth}} = [\exp(\hbar\omega/\kappa_B T) - 1]^{-1}$ , where  $\kappa_B$  is the Boltzmann constant and  $T$  is the environment temperature.

By enhancing the atom-phonon interaction we find phonon blockade in the one-cavity system. To observe quantum effects from a single phonon, we numerically calculate the mechanical-mode steady-state equal-time

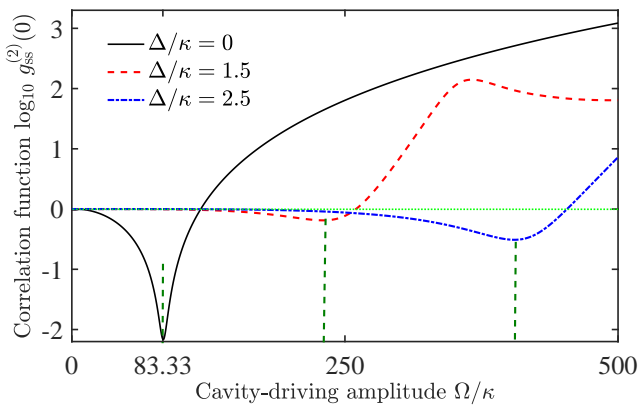


FIG. 4. (Color online) Correlation function  $\log_{10} g_{ss}^{(2)}(0)$  versus the optical driving amplitude  $\Omega$  with different detunings  $\Delta$  between the mechanical mode and the corresponding driving field in the one-cavity system. The parameters used here are the same as in Fig. 2.

second-order correlation function

$$g_{ss}^{(2)}(0) = \frac{\langle \hat{b}^\dagger \hat{b}^\dagger \hat{b} \hat{b} \rangle}{\langle \hat{b}^\dagger \hat{b} \rangle^2}, \quad (7)$$

using the master equation in the basis of Fock states. The numerical results shown in Fig. 3 clearly demonstrate that, assuming  $\Delta = 0$ , the strongest phonon blockade appears when  $\Omega/\kappa = 83.33$ . At other points of the optical driving amplitude, the value of the correlation function becomes much larger even if the phonon blockade still exists. The optimal point corresponds to

$$G = \frac{1}{2} \sqrt{\kappa(\kappa + \gamma)}, \quad (8)$$

which is derived in Ref. [66] from the wave function of the truncated low-dimensional Hilbert space. Figure 4 shows the influence of the detuning  $\Delta$  on the correlation function  $g_{ss}^{(2)}(0)$ , validating the optimal conditions specified above.

Considering the energy of the system in the rotating frame, the appearance of high-quality phonon blockade (as described by strong phonon antibunching) is due to the resonance between a single phonon and the shifted frequency of the atom. Then the atom-phonon interaction induces the energy-level splitting of the system, which blockades a second phonon entering into the system.

#### IV. PHONON BLOCKADE IN THE TWO-CAVITY SYSTEM

In this section, we analyze the atom-phonon-phonon interaction resulting from the optomechanical coupling in the two-cavity system, shown in Fig. 1(c). Then we derive the atom-phonon interaction, which is not only enhanced by the average photon number, but also by

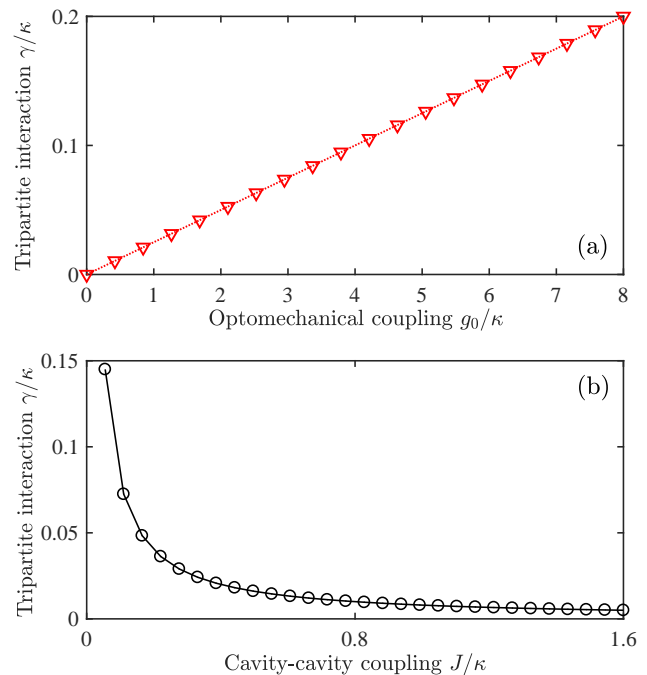


FIG. 5. (Color online) The atom-phonon-phonon interaction rate  $\gamma$  in the two-cavity system versus: (a) the optomechanical coupling strength  $g_0$  with  $J/2\pi = 4$  MHz, (b) the coupling strength of the two cavities  $J$  with  $g_0/2\pi = 2$  MHz. Here  $g/2\pi = 0.4$  MHz,  $J_m/2\pi = 0.01$  MHz, and all the other parameters are the same as in Fig. 2.

the atom-phonon-phonon interaction rate  $\gamma$ . Finally, we predict phonon blockade in the two-cavity system.

The schematic diagram of the two-cavity system is shown in Fig. 1(c): two identical optomechanical cavities (oscillators)  $\hat{a}_l$  ( $\hat{b}_l$ ) and  $\hat{a}_r$  ( $\hat{b}_r$ ) are linearly coupled together with coupling rate  $J$  ( $J_m$ ). The atom couples to the left cavity with coupling rate  $g$ . The left mechanical mode is driven by a weak driving field with resonant frequency  $\omega_m$  and amplitude  $\varepsilon$ . Then the Hamiltonian, representing the total two-cavity system reads as

$$\begin{aligned} \hat{H}_{2\text{tot}}/\hbar = & [\omega_c - g_0(\hat{b}_l^\dagger + \hat{b}_l)]\hat{a}_l^\dagger \hat{a}_l + [\omega_c - g_0(\hat{b}_r^\dagger + \hat{b}_r)]\hat{a}_r^\dagger \hat{a}_r \\ & + \frac{\omega_a}{2} \hat{\sigma}_z + \omega_m(\hat{b}_l^\dagger \hat{b}_l + \hat{b}_r^\dagger \hat{b}_r) + J(\hat{a}_r^\dagger \hat{a}_l + \hat{a}_l^\dagger \hat{a}_r) \\ & + J_m(\hat{b}_l^\dagger \hat{b}_r + \hat{b}_r^\dagger \hat{b}_l) + g(\hat{\sigma}_+ \hat{a}_l + \hat{\sigma}_- \hat{a}_l^\dagger) \\ & + \varepsilon(\hat{b}_l^\dagger e^{-i\omega_m t} + \hat{b}_l e^{i\omega_m t}). \end{aligned} \quad (9)$$

To better analyze the physical mechanism described by this Hamiltonian, we introduce the mechanical supermode annihilation operators

$$\hat{b}_\pm = \frac{1}{\sqrt{2}}(\hat{b}_l \pm \hat{b}_r). \quad (10)$$

The supermode  $\hat{b}_+$  interacts with the left and right cavity modes with an equal coupling strength  $-g_0/\sqrt{2}$ , while the supermode  $\hat{b}_-$  interacts with these cavities with an equal and opposite coupling strength  $\mp g_0/\sqrt{2}$ . Then we

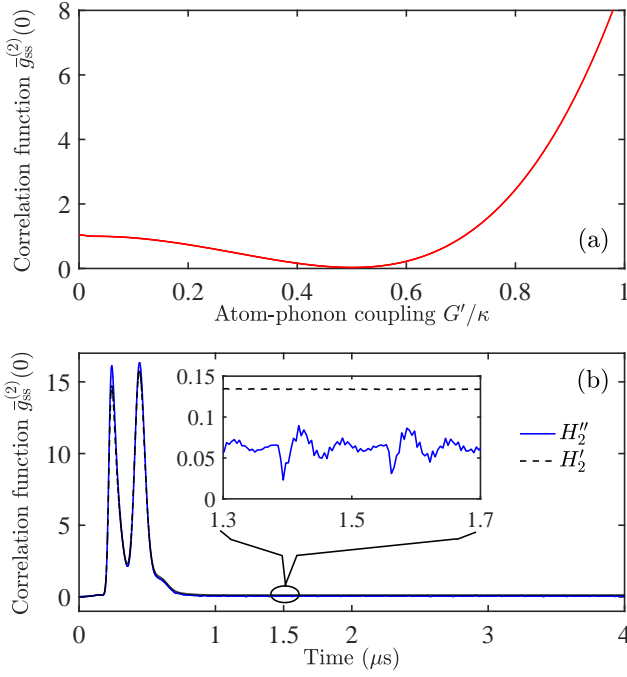


FIG. 6. (Color online) The second-order correlation function  $\bar{g}_{ss}^{(2)}(0)$ , given by Eq. (19) for the mechanical supermode  $\hat{b}_-$ , versus: (a) the atom-phonon coupling strength  $G'$  and (b) time  $t$ , in the two-cavity system. Here  $G' = 0.5\kappa$ ,  $\sqrt{n_+} = 51$ ,  $\sqrt{n_-} = 1$ , and  $\varepsilon = 0.03\kappa$ , while all the other parameters are the same as in Fig. 2.

can effectively omit the mode  $\hat{b}_+$  from Hamiltonian (9). Moreover, the condition  $J_m \ll \omega_m$ , enables us to safely neglect the terms containing  $J_m$ . Under the condition of quasi-static approximation [59] for  $\hat{\delta}_b$ , the optical parts in Hamiltonian (9) can be diagonalized in the rotating frame with frequency  $\omega_c$ . Thus, the effective Hamiltonian becomes

$$\begin{aligned} \hat{H}_2/\hbar = & \sqrt{\hat{\delta}_b^2 + J^2} \hat{a}_+^\dagger \hat{a}_+ - \sqrt{\hat{\delta}_b^2 + J^2} \hat{a}_-^\dagger \hat{a}_- + \frac{\omega_m}{2} \hat{\sigma}_z \\ & + g\hat{\alpha}(\hat{\sigma}_+ \hat{a}_+ + \hat{\sigma}_- \hat{a}_+^\dagger) + g\hat{\beta}(\hat{\sigma}_+ \hat{a}_- + \hat{\sigma}_- \hat{a}_-^\dagger) \\ & + \omega_m \hat{b}_-^\dagger \hat{b}_- + \frac{1}{\sqrt{2}} \varepsilon (\hat{b}_-^\dagger e^{-i\omega_m t} + \hat{b}_- e^{i\omega_m t}), \end{aligned} \quad (11)$$

where the contribution of

$$\hat{\delta}_b = \frac{g_0}{\sqrt{2}} (\hat{b}^\dagger + \hat{b}), \quad |\delta_b| \ll J, \quad (12)$$

can be neglected safely in the frequencies of optical supermodes. And

$$\hat{\alpha} = J \left[ \left( \sqrt{\hat{\delta}_b^2 + J^2} + \hat{\delta}_b \right)^2 + J^2 \right]^{-1/2}, \quad (13a)$$

$$\hat{\beta} = \frac{\hat{\alpha}}{J} \left( \sqrt{\hat{\delta}_b^2 + J^2} + \hat{\delta}_b \right). \quad (13b)$$

Meanwhile, we expand  $\hat{\alpha}$  and  $\hat{\beta}$  to first order in the small

parameter  $\hat{\delta}_b/J$  to obtain:

$$\hat{\alpha} = \frac{1}{\sqrt{2}} \left( 1 - \frac{\hat{\delta}_b}{2J} \right), \quad \hat{\beta} = \frac{1}{\sqrt{2}} \left( 1 + \frac{\hat{\delta}_b}{2J} \right). \quad (14)$$

Inserting Eq. (14) into Hamiltonian (11), we obtain the following tripartite atom-photon-phonon interaction term

$$\gamma (\hat{b}_-^\dagger + \hat{b}_-) [\hat{\sigma}_+ (\hat{a}_+ - \hat{a}_-) + \hat{\sigma}_- (\hat{a}_+ - \hat{a}_-)], \quad (15)$$

with the effective interaction rate  $\gamma = gg_0/(4J)$ . This illustrates that we can derive the atom-photon-phonon interaction from the standard optomechanical coupling.

Let us rewrite the optical supermode operators as  $\hat{a}_+ = \sqrt{n_+} + \delta\hat{a}_+$  and  $\hat{a}_- = \sqrt{n_-} + \delta\hat{a}_-$ . After inserting these operators and Eq. (14) into Hamiltonian (11), under the rotating-wave approximation, the Hamiltonian reduces to

$$\begin{aligned} \hat{H}_2'/\hbar = & -G' (\hat{\sigma}_+ \hat{b}_- + \hat{\sigma}_- \hat{b}_-^\dagger) + \frac{\varepsilon}{\sqrt{2}} (\hat{b}_-^\dagger + \hat{b}_-) \\ & + \frac{g}{\sqrt{2}} \frac{G'}{\gamma} (\hat{\sigma}_+ e^{i\omega_m t} + \hat{\sigma}_- e^{-i\omega_m t}), \end{aligned} \quad (16)$$

where  $G' = \gamma(\sqrt{n_+} - \sqrt{n_-})$ , is the atom-phonon coupling strength. Note that the atom-phonon interaction is not only modulated by the average photon numbers of the supermodes, but also by the atom-photon-phonon interaction rate  $\gamma$ . Since  $\sqrt{n_+}$  is much larger than  $\sqrt{n_-}$ , we can efficiently enhance the atom-phonon coupling through the average photon numbers of the supermodes. Also, the atom-photon-phonon coupling rate here is related to the optomechanical interaction rate  $g_0$  and the cavities-coupling rate  $J$  when the atom-photon interaction rate is fixed. It is obvious that the atom-photon-phonon interaction can reach a very large value if  $g_0$  is large and  $J$  is small enough (for feasible values of parameters) in the system. The results are shown in Fig. 5: keeping  $J$  fixed, the tripartite interaction rate varies linearly with the optomechanical interaction and inversely proportional to the cavities coupling when other parameters are fixed. These illustrate that the atom-phonon interaction can be controlled with more parameters in the two-cavity system. Simultaneously, it also improves the feasibility of future experiments exploring this regime.

Under the condition

$$\frac{g}{\omega_m} (\sqrt{n_+} - \sqrt{n_-}) \ll 1, \quad (17)$$

the third term in the Hamiltonian given in Eq. (16) is quickly oscillating and can be safely omitted, which results in

$$\hat{H}_2''/\hbar = -G' (\hat{\sigma}_+ \hat{b}_- + \hat{b}_-^\dagger \hat{\sigma}_-) + \frac{1}{\sqrt{2}} \varepsilon (\hat{b}_-^\dagger + \hat{b}_-). \quad (18)$$

Just as in the one-cavity system, we demonstrate the property of the steady-state phonon statistics. The property of phonon statistics is expressed by a steady-state

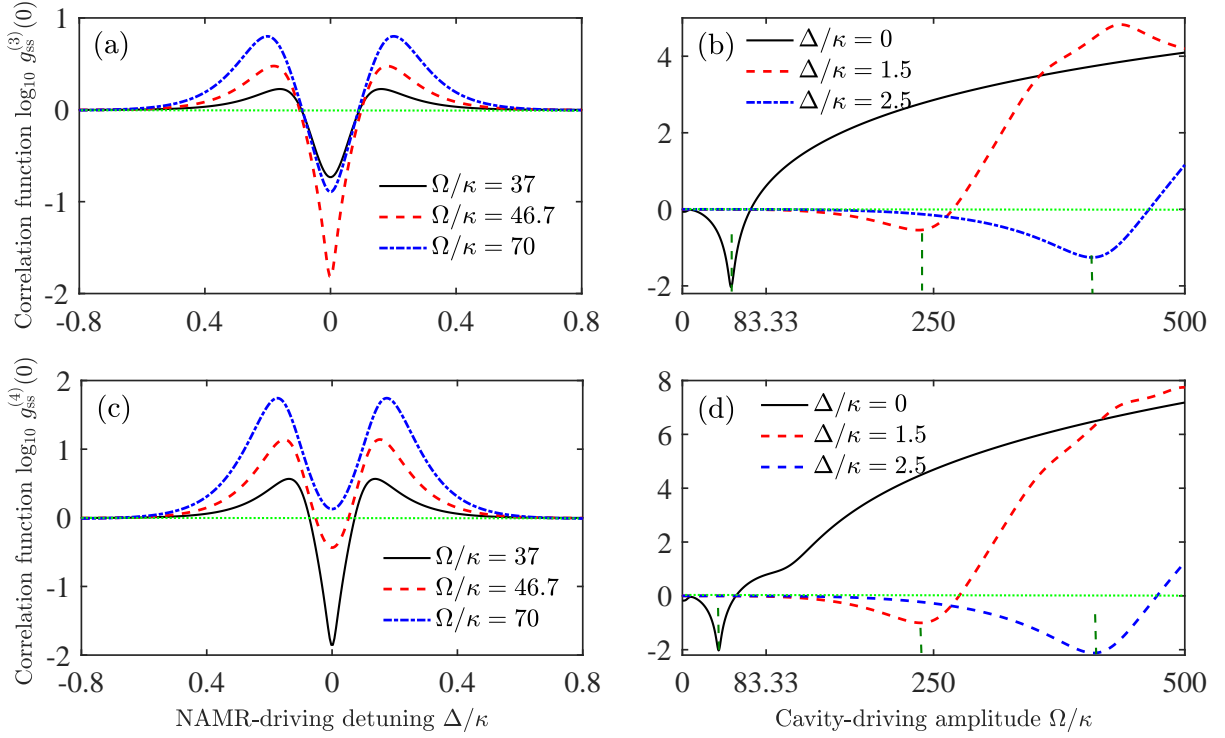


FIG. 7. (Color online) (a,b) Third- and (c,d) fourth-order correlation functions  $\log_{10} g_{ss}^{(n)}(0)$  of the generated phonon steady states versus: (a,c) the detuning  $\Delta$  between the NAMR and the corresponding driving field and (b,d) the optical driving amplitude  $\Omega$  under different conditions in the one-cavity system. All the parameters are the same as in Figs. 3 and 4.

TABLE I. Different kinds of phonon blockade (PB) corresponding to the regions of different detunings shown in Fig. 8. Criteria for non-standard PB and phonon-induced tunneling are given in Eqs. (21) and (22), respectively.

| No. | Region | Correlation functions                                     | Effect                   | Detuning $ \Delta /\kappa$ |
|-----|--------|---|--------------------------|----------------------------|
| 1   | A      | $1 > g_{ss}^{(2)}(0) > g_{ss}^{(4)}(0) > g_{ss}^{(3)}(0)$ | standard PB              | (0, 0.030)                 |
| 2   | B      | $1 > g_{ss}^{(4)}(0) > g_{ss}^{(2)}(0) > g_{ss}^{(3)}(0)$ | standard PB              | (0.030, 0.053)             |
| 3   | C      | $g_{ss}^{(4)}(0) > 1 > g_{ss}^{(2)}(0) > g_{ss}^{(3)}(0)$ | non-standard PB          | (0.053, 0.088)             |
| 4   | D      | $g_{ss}^{(4)}(0) > 1 > g_{ss}^{(3)}(0) > g_{ss}^{(2)}(0)$ | non-standard PB          | (0.088, 0.098)             |
| 5   | E      | $g_{ss}^{(4)}(0) > g_{ss}^{(3)}(0) > 1 > g_{ss}^{(2)}(0)$ | non-standard PB          | (0.098, 0.124)             |
| 6   | F      | $g_{ss}^{(4)}(0) > g_{ss}^{(3)}(0) > g_{ss}^{(2)}(0) > 1$ | phonon-induced tunneling | (0.124, 0.6)               |

equal-time second-order correlation function for the mechanical supermode  $\hat{b}_-$ , as

$$\bar{g}_{ss}^{(2)}(0) = \frac{\langle \hat{b}_-^\dagger \hat{b}_-^\dagger \hat{b}_- \hat{b}_- \rangle}{\langle \hat{b}_-^\dagger \hat{b}_- \rangle^2}. \quad (19)$$

Here the mechanical supermode  $\hat{b}_-$  is the linear superposition of the mechanical operators  $\hat{b}_l$  and  $\hat{b}_r$ . As for the two driven and coupled semipermeable resonators, phonon blockade can be observed even more easily than that in the one-cavity system. This results from multi-path interference, which is the mechanism of UPB.

We can clearly verify the theory analysis shown above via numerical calculations. As shown in Fig. 6(a), the strongest phonon blockade appears still at the same optimal point, which coincides with the corresponding result

in the one-cavity system. This proves that the quantum characteristics of the mechanical modes and the mechanical supermodes are not changed in the one- or two-cavity systems. To check the validity of the approximation from  $\hat{H}'_2$  to  $\hat{H}''_2$ , we show in Fig. 6(b) the evolution of the correlation functions  $\bar{g}_{ss}^{(2)}(0)$  governed by the Hamiltonians  $\hat{H}'_2$  and  $\hat{H}''_2$ . From the inset of Fig. 6(b), we can see that the blue curve (corresponding to  $\hat{H}''_2$ ) is slightly lower than exact numerical calculation, the black dashed curve (corresponding to  $\hat{H}'_2$ ), illustrating that we have made a valid approximation. Note that these slight differences are visible only in the magnified inset of Fig. 6(b). Moreover, the steady states of the studied evolution almost coincide with the value in Fig. 6(a) at the optimal point.

In the two-cavity system, Hamiltonian (9), includes di-

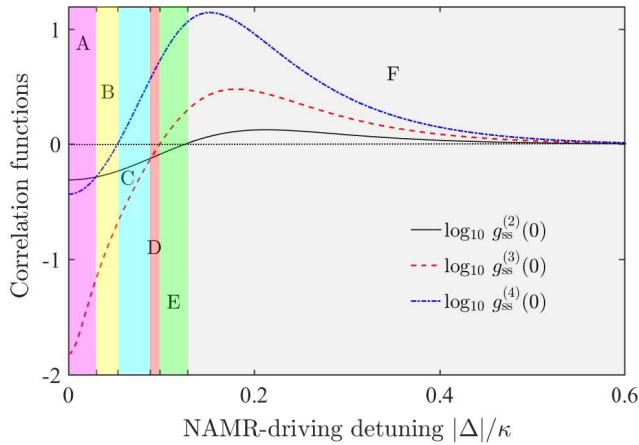


FIG. 8. (Color online) Correlation functions  $\log_{10} g_{ss}^{(n)}(0)$  for  $n = 2, 3, 4$  of the generated phonon steady states as a function of the absolute value of the detuning  $|\Delta|$  between the NAMR and the corresponding driving field in the one-cavity system. We assume that  $\Omega/\kappa = 46.7$  and all the other parameters are the same as in Fig. 7. The regions marked A, ..., F correspond to different kinds of PB and phonon-induced tunneling, as summarized in Table I.

rect atom-photon and photon-phonon interaction terms. The atom and NAMR interact with each other indirectly through the common cavity field (a quantum bus). Thus, we can interpret the predicted phonon blockade in the two-cavity system as induced by an indirect atom-phonon interaction. Such an interpretation of phonon blockade for a single-cavity system, would be less justified, because the original Hamiltonian in Eq. (1), already includes a direct atom-photon-phonon interaction. Note that the effective Hamiltonian, given in Eq. (18), also includes apparently a direct tripartite atom-photon-phonon term. This interaction can be interpreted as a bipartite atom-phonon interaction, when the influence of the cavity field is treated as a classical parameter and incorporated in the coupling constant  $G'$ .

## V. HIGHER-ORDER PHONON-NUMBER CORRELATIONS

It is known that not all phonon states with  $g_{ss}^{(2)}(0) < 1$  correspond to standard phonon blockade [67]. By analyzing higher-order correlation functions, we can perform a more insightful analysis of PB generated in our models. Because the physical mechanisms of PB are very similar in the one- and two-cavity systems, we only analyze here the one-cavity model.

Higher-order phonon-number steady-state correlation functions can be defined by:

$$g_{ss}^{(n)}(0) = \frac{\langle (\hat{b}^\dagger)^n \hat{b}^n \rangle}{\langle \hat{b}^\dagger \hat{b} \rangle^n}, \quad (20)$$

as a generalization of  $g_{ss}^{(2)}(0)$ . We recall that standard

PB occurs if  $g_{ss}^{(n)}(0) < 1$ , not only for  $n = 2$  but also for higher orders  $n$ . Thus, one can talk about *non-standard* PB if

$$g_{ss}^{(2)}(0) < 1 \quad \text{and} \quad g_{ss}^{(n)}(0) > 1 \quad (21)$$

for some  $n > 1$ . For numerical convenience, we refer to standard PB if  $g_{ss}^{(n)}(0) < 1$  for  $n = 2, 3, 4$  only. Of course, one can find that in some cases such PB is not really standard by calculating  $g_{ss}^{(n)}(0)$  for  $n \geq 5$ . Moreover, one can find other classifications of standard and non-standard PB by applying more refined criteria, like those in Refs. [67–69]. Note that PB described by Eq. (21) is also referred to as *unconventional* PB (regime) [64]. It is clear that this meaning of UPB refers to unconventional properties of the generated light via PB. Recall that the term UPB used in the title of this paper and explained in its Introduction refers to an unconventional mechanism (based on multipath interference) for creating or enhancing PB [16, 63]. Thus, to avoid confusion, we use the term non-standard PB (rather than UPB) for mechanical states described by Eq. (21).

Moreover, we refer to *phonon-induced tunneling* if the following conditions are satisfied

$$g_{ss}^{(4)}(0) > g_{ss}^{(3)}(0) > g_{ss}^{(2)}(0) > 1. \quad (22)$$

This effect is an analogue of *photon-induced tunneling* studied in, e.g., Ref. [70] (see also references cited therein). Note that Ref. [70] defines this photon tunneling via a weaker condition [i.e.,  $g_{ss}^{(3)}(0) > g_{ss}^{(2)}(0) > 1$ ]. If  $g_{ss}^{(4)}(0) < 1$  [ $g_{ss}^{(5)}(0) < 1$ ], one can interpret such tunneling as three-PB (four-PB), in analogy to Refs. [67, 71]. For simplicity, in this work, we have neither calculated  $g_{ss}^{(n)}(0)$  for  $n = 5, \dots$  nor searched for multi-PB.

Our numerical results for  $g_{ss}^{(3)}(0)$  and  $g_{ss}^{(4)}(0)$  are shown in Fig. 7, which can be easily compared with the results for  $g_{ss}^{(2)}(0)$  shown in Figs. 3 and 4. A more explicit comparison of  $g_{ss}^{(n)}(0)$  (for  $n = 2, 3, 4$ ) as a function of the detuning  $|\Omega|$  (in units of the atom-damping rate  $\kappa$ ) is shown in Fig. 8. These results, as summarized in Table I, reveal regions of specific interrelations between the correlation functions  $g_{ss}^{(n)}(0)$  of different orders  $n$ . Each such region corresponds to a specific phonon-number-correlation effect including standard and nonstandard PB, as well as phonon-induced tunneling of phonons.

## VI. CONCLUSIONS

We have provided a method to generate strong phonon blockade in hybrid one-cavity and two-cavity optomechanical systems, which are originally in the weak-coupling regime. Our approach utilizes a modulated atom-phonon interaction obtained from the tripartite atom-photon-phonon interaction. We have shown that this atom-phonon coupling strength can be enhanced by

adjusting the driving-field amplitude and frequency, in the single-cavity optomechanical system, and the mechanical coupling strength in the two-cavity case. We presented optimal parameter regimes for realizing high-quality phonon blockade. Based on the original Hamiltonian, we also have verified the validity of the approximations used in our work. By comparing phonon-number correlation functions  $g_{ss}^{(n)}(0)$  of different orders  $n = 2, 3, 4$ , for given mechanical steady states in the one-cavity system, we found different types of standard and non-standard phonon blockade, as well as phonon-induced tunneling.

This study provides a new route to produce high-quality phonon blockade using the nonlinearity induced by an atom (qubit) [25, 40, 43, 44, 56, 72] in optomechanical hybrid systems, and has potential applications

for quantum technologies.

## ACKNOWLEDGMENTS

This work is supported by the National Key R&D Program of China grant 2016YFA0301203, the National Science Foundation of China (Grant Nos. 11374116, 11574104 and 11375067). FN is partially supported by the MURI Center for Dynamic Magneto-Optics via the AFOSR Award No. FA9550-14-1-0040, the Army Research Office (ARO) under grant number 73315PH, the AOARD grant No. FA2386-18-1-4045, the CREST Grant No. JPMJCR1676, the IMPACT program of JST, the RIKEN-AIST Challenge Research Fund, and the JSPS-RFBR grant No. 17-52-50023. AM and FN acknowledge also a grant from the John Templeton Foundation.

- 
- [1] M. Aspelmeyer, T. J. Kippenberg, and F. Marquardt, “Cavity optomechanics,” *Rev. Mod. Phys.* **86**, 1391–1452 (2014).
- [2] F. Marquardt and S. M. Girvin, “Trend: Optomechanics,” *Physics* **2**, 40 (2009).
- [3] M. Aspelmeyer, P. Meystre, and K. Schwab, “Quantum optomechanics,” *Physics* **65**, 29 (2012).
- [4] P. Meystre, “A short walk through quantum optomechanics,” *Ann. Phys. (Berlin)* **525**, 215–233 (2013).
- [5] T. J. Kippenberg and K. J. Vahala, “Cavity optomechanics: Back-action at the mesoscale,” *Science* **321**, 1172–1176 (2008).
- [6] C. Dong, V. Fiore, M. C. Kuzuk, and H. Wang, “Optomechanical dark mode,” *Science* **338**, 1609–1613 (2012).
- [7] X. M. H. Huang, C. A. Zorman, M. Mehregany, and M. L. Roukes, “Nanoelectromechanical systems: Nanodevice motion at microwave frequencies,” *Nature (London)* **421**, 496–496 (2003).
- [8] R. G. Knobel and A. N. Cleland, “Nanometre-scale displacement sensing using a single electron transistor,” *Nature* **424**, 291–293 (2003).
- [9] K. L. Ekinci and M. L. Roukes, “Nanoelectromechanical systems,” *Rev. Sci. Instrum.* **76**, 061101 (2005).
- [10] K. C. Schwab and M. L. Roukes, “Putting mechanics into quantum mechanics,” *Phys. Today* **58**, 36 (2005).
- [11] V. B. Braginsky and F. Ya. Khalili, *Quantum Measurements* (Cambridge University Press, Cambridge, England, 1992).
- [12] V. B. Braginsky and F. Y. Khalili, “Low noise rigidity in quantum measurements,” *Phys. Lett. A* **257**, 241–246 (1999).
- [13] C. Weedbrook, S. Pirandola, R. García-Patrón, N. J. Cerf, T. C. Ralph, J. H. Shapiro, and S. Lloyd, “Gaussian quantum information,” *Rev. Mod. Phys.* **84**, 621–669 (2012).
- [14] C. H. Bennett and D. P. DiVincenzo, “Quantum information and computation,” *Nature (London)* **404**, 247–255 (2000).
- [15] N. Gisin and R. Thew, “Quantum information and computation,” *Nat. Photon* **1**, 165–171 (2007).
- [16] X. Gu, A. F. Kockum, A. Miranowicz, Y.-x. Liu, and F. Nori, “Microwave photonics with superconducting quantum circuits,” *Phys. Rep.* **718–719**, 1–102 (2017).
- [17] L. Tian and H. J. Carmichael, “Quantum trajectory simulations of two-state behavior in an optical cavity containing one atom,” *Phys. Rev. A* **46**, R6801–R6804 (1992).
- [18] W. Leoński and R. Tanaś, “Possibility of producing the one-photon state in a kicked cavity with a nonlinear Kerr medium,” *Phys. Rev. A* **49**, R20–R23 (1994).
- [19] A. Imamoglu, H. Schmidt, G. Woods, and M. Deutsch, “Erratum: Strongly interacting photons in a nonlinear cavity,” *Phys. Rev. Lett.* **81**, 2836–2836 (1998).
- [20] W. Leoński and A. Miranowicz, “Kerr nonlinear coupler and entanglement,” *J. Opt. B* **6**, S37 (2004).
- [21] A. Miranowicz and W. Leoński, “Two-mode optical state truncation and generation of maximally entangled states in pumped nonlinear couplers,” *J. Phys. B* **39**, 1683 (2006).
- [22] T. C. H. Liew and V. Savona, “Single photons from coupled quantum modes,” *Phys. Rev. Lett.* **104**, 183601 (2010).
- [23] M. Bamba, A. Imamoglu, I. Carusotto, and C. Ciuti, “Origin of strong photon antibunching in weakly nonlinear photonic molecules,” *Phys. Rev. A* **83**, 021802 (2011).
- [24] A. Miranowicz, J. Bajer, N. Lambert, Y.-x. Liu, and F. Nori, “Tunable multiphonon blockade in coupled nanomechanical resonators,” *Phys. Rev. A* **93**, 013808 (2016).
- [25] X. Wang, A. Miranowicz, H.-R. Li, and F. Nori, “Method for observing robust and tunable phonon blockade in a nanomechanical resonator coupled to a charge qubit,” *Phys. Rev. A* **93**, 063861 (2016).
- [26] K. M. Birnbaum, A. Boca, R. Miller, A. D. Boozer, T. E. Northup, and H. J. Kimble, “Photon blockade in an optical cavity with one trapped atom,” *Nature (London)* **436**, 87–90 (2005).

- [27] J.-Q. Liao and F. Nori, “Photon blockade in quadratically coupled optomechanical systems,” *Phys. Rev. A* **88**, 023853 (2013).
- [28] P. Rabl, “Photon blockade effect in optomechanical systems,” *Phys. Rev. Lett.* **107**, 063601 (2011).
- [29] F. L. Semião, K. Furuya, and G. J. Milburn, “Kerr nonlinearities and nonclassical states with superconducting qubits and nanomechanical resonators,” *Phys. Rev. A* **79**, 063811 (2009).
- [30] N. Didier, S. Pugnetti, Y. M. Blanter, and R. Fazio, “Detecting phonon blockade with photons,” *Phys. Rev. B* **84**, 054503 (2011).
- [31] L. C. G. Góvia, E. J. Pritchett, and F. K. Wilhelm, “Generating nonclassical states from classical radiation by subtraction measurements,” *New J. Phys.* **16**, 045011 (2014).
- [32] V. C. Usenko, L. Ruppert, and R. Filip, “Quantum communication with macroscopically bright nonclassical states,” *Opt. Express* **23**, 31534–31543 (2015).
- [33] X. Hu and F. Nori, “Squeezed phonon states: Modulating quantum fluctuations of atomic displacements,” *Phys. Rev. Lett.* **76**, 2294–2297 (1996).
- [34] X. Hu and F. Nori, “Quantum phonon optics: Coherent and squeezed atomic displacements,” *Phys. Rev. B* **53**, 2419–2424 (1996).
- [35] X. Hu and F. Nori, “Phonon squeezed states generated by second-order Raman scattering,” *Phys. Rev. Lett.* **79**, 4605–4608 (1997).
- [36] X. Hu and F. Nori, “Phonon squeezed states: quantum noise reduction in solids,” *Physica B: Condensed Matter* **263–264**, 16–29 (1999).
- [37] A. Facon, E.-K. Dietsche, D. Grosso, S. Haroche, J.-M. Raimond, M. Brune, and S. Gleyzes, “A sensitive electrometer based on a Rydberg atom in a Schrödinger-cat state,” *Nature (London)* **535**, 262–265 (2016).
- [38] Y.-x. Liu, A. Miranowicz, Y. B. Gao, J. Bajer, C. P. Sun, and F. Nori, “Qubit-induced phonon blockade as a signature of quantum behavior in nanomechanical resonators,” *Phys. Rev. A* **82**, 032101 (2010).
- [39] K. Hammerer, M. Wallquist, C. Genes, M. Ludwig, F. Marquardt, P. Treutlein, P. Zoller, J. Ye, and H. J. Kimble, “Strong coupling of a mechanical oscillator and a single atom,” *Phys. Rev. Lett.* **103**, 063005 (2009).
- [40] S. Ashhab and F. Nori, “Qubit-oscillator systems in the ultrastrong-coupling regime and their potential for preparing nonclassical states,” *Phys. Rev. A* **81**, 042311 (2010).
- [41] I. Buluta, S. Ashhab, and F. Nori, “Natural and artificial atoms for quantum computation,” *Rep. Prog. Phys.* **74**, 104401 (2011).
- [42] Z.-L. Xiang, S. Ashhab, J. Q. You, and F. Nori, “Hybrid quantum circuits: Superconducting circuits interacting with other quantum systems,” *Rev. Mod. Phys.* **85**, 623–653 (2013).
- [43] W. Qin, X. Wang, A. Miranowicz, Z. Zhong, and F. Nori, “Heralded quantum controlled-phase gates with dissipative dynamics in macroscopically distant resonators,” *Phys. Rev. A* **96**, 012315 (2017).
- [44] S. Singh and P. Meystre, “Atomic probe Wigner tomography of a nanomechanical system,” *Phys. Rev. A* **81**, 041804 (2010).
- [45] K. Hammerer, M. Wallquist, C. Genes, M. Ludwig, F. Marquardt, P. Treutlein, P. Zoller, J. Ye, and H. J. Kimble, “Strong coupling of a mechanical oscillator and a single atom,” *Phys. Rev. Lett.* **103**, 063005 (2009).
- [46] M. Khudaverdyan, W. Alt, I. Dotsenko, T. Kampschulte, K. Lenhard, A. Rauschenbeutel, S. Reick, K. Schörner, A. Widera, and D. Meschede, “Controlled insertion and retrieval of atoms coupled to a high-finesse optical resonator,” *New J. Phys.* **10**, 073023 (2008).
- [47] X. X. Yi, L. Zhou, and H. S. Song, “Entangling two cavity modes via a two-photon process,” *J. Phys. A* **37**, 5477 (2004).
- [48] J. Q. You and F. Nori, “Atomic physics and quantum optics using superconducting circuits,” *Nature* **474**, 589–597 (2011).
- [49] I. Mahboob, H. Okamoto, K. Onomitsu, and H. Yamaguchi, “Two-mode thermal-noise squeezing in an electromechanical resonator,” *Phys. Rev. Lett.* **113**, 167203 (2014).
- [50] M. Blencowe, “Quantum electromechanical systems,” *Phys. Rep.* **395**, 159–222 (2004).
- [51] X.-Y. Lü, H. Jing, J.-Y. Ma, and Y. Wu, “ $\mathcal{PT}$ -symmetry-breaking chaos in optomechanics,” *Phys. Rev. Lett.* **114**, 253601 (2015).
- [52] T.-S. Yin, X.-Y. Lü, L.-L. Zheng, M. Wang, S. Li, and Y. Wu, “Nonlinear effects in modulated quantum optomechanics,” *Phys. Rev. A* **95**, 053861 (2017).
- [53] X.-Y. Lü, J.-Q. Liao, L. Tian, and F. Nori, “Steady-state mechanical squeezing in an optomechanical system via duffing nonlinearity,” *Phys. Rev. A* **91**, 013834 (2015).
- [54] P.-B. Li, Z.-L. Xiang, P. Rabl, and F. Nori, “Hybrid quantum device with nitrogen-vacancy centers in diamond coupled to carbon nanotubes,” *Phys. Rev. Lett.* **117**, 015502 (2016).
- [55] A. D. O’Connell, M. Hofheinz, M. Ansmann, R. C. Bialczak, M. Lenander, E. Lucero, M. Neeley, D. Sank, H. Wang, M. Weides, J. Wenner, J. M. Martinis, and A. N. Cleland, “Quantum ground state and single-phonon control of a mechanical resonator,” *Nature* **464**, 697 (2010).
- [56] A. N. Cleland and M. R. Geller, “Superconducting qubit storage and entanglement with nanomechanical resonators,” *Phys. Rev. Lett.* **93**, 070501 (2004).
- [57] D. A. Golter, T. Oo, M. Amezcu, K. A. Stewart, and H. Wang, “Optomechanical quantum control of a nitrogen-vacancy center in diamond,” *Phys. Rev. Lett.* **116**, 143602 (2016).
- [58] I. Wilson-Rae, P. Zoller, and A. Imamoglu, “Laser cooling of a nanomechanical resonator mode to its quantum ground state,” *Phys. Rev. Lett.* **92**, 075507 (2004).
- [59] M. Cotrufo, A. Fiore, and E. Verhagen, “Coherent atom-phonon interaction through mode field coupling in hybrid optomechanical systems,” *Phys. Rev. Lett.* **118**, 133603 (2017).
- [60] A. Miranowicz, J. Bajer, M. Paprzycka, Y.-x. Liu, A. M. Zagoskin, and F. Nori, “State-dependent photon blockade via quantum-reservoir engineering,” *Phys. Rev. A* **90**, 033831 (2014).
- [61] Y.-x. Liu, X.-W. Xu, A. Miranowicz, and F. Nori, “From blockade to transparency: Controllable photon transmission through a circuit-qed system,” *Phys. Rev. A* **89**, 043818 (2014).
- [62] H. Wang, X. Gu, Y.-x. Liu, A. Miranowicz, and F. Nori, “Tunable photon blockade in a hybrid system consisting of an optomechanical device coupled to a two-level system,” *Phys. Rev. A* **92**, 033806 (2015).
- [63] H. Flayac and V. Savona, “Unconventional photon block-

- ade,” *Phys. Rev. A* **96** (2017).
- [64] M. Radulaski, K. A. Fischer, K. G. Lagoudakis, J. L. Zhang, and J. Vučković, “Photon blockade in two-emitter-cavity systems,” *Phys. Rev. A* **96** (2017).
- [65] J. Zhang, B. Peng, Ş. K. Özdemir, Y.-x. Liu, H. Jing, X.-y. Lü, Y.-l. Liu, L. Yang, and F. Nori, “Giant nonlinearity via breaking parity-time symmetry: A route to low-threshold phonon diodes,” *Phys. Rev. B* **92**, 115407 (2015).
- [66] X.-W. Xu, A.-X. Chen, and Y.-x. Liu, “Phonon blockade in a nanomechanical resonator resonantly coupled to a qubit,” *Phys. Rev. A* **94**, 063853 (2016).
- [67] C. Hamsen, K. N. Tolazzi, T. Wilk, and G. Rempe, “Two-photon blockade in an atom-driven cavity qed system,” *Phys. Rev. Lett.* **118**, 133604 (2017).
- [68] J. C. L. Carreno, E. Z. Casalengua, E. del Valle, and F. P. Laussy, “Criterion for single photon sources,” [arXiv:1610.06126](https://arxiv.org/abs/1610.06126).
- [69] A. Miranowicz, M. Bartkowiak, X. Wang, Y. Liu, and F. Nori, “Testing nonclassicality in multimode fields: A unified derivation of classical inequalities,” *Phys. Rev. A* **82** (2010).
- [70] A. Rundquist, M. Bajcsy, A. Majumdar, T. Sarmiento, K. Fischer, K. G. Lagoudakis, S. Buckley, A. Y. Pigott, and J. Vučković, “Nonclassical higher-order photon correlations with a quantum dot strongly coupled to a photonic-crystal nanocavity,” *Phys. Rev. A* **90** (2014).
- [71] A. Miranowicz, M. Paprzycka, Y.-x. Liu, J. Bajer, and F. Nori, “Two-photon and three-photon blockades in driven nonlinear systems,” *Phys. Rev. A* **87**, 023809 (2013).
- [72] T. Ramos, V. Sudhir, K. Stannigel, P. Zoller, and T. J. Kippenberg, “Nonlinear quantum optomechanics via individual intrinsic two-level defects,” *Phys. Rev. Lett.* **110**, 193602 (2013).